PUBLICATIONS OF THE ASTRONOMICAL SOCIETY OF THE PACIFIC, 112:1542–1548, 2000 December

Modified Strömgren Sphere

PETER R. MCCULLOUGH[1]
Astronomy Department, University of Illinois, Urbana, IL 61801; pmcc@astro.uiuc.edu

Received 2000 August 15; accepted 2000 August 18

ABSTRACT. A Strömgren sphere is the theoretical result of an ionizing source such as a hot star placed in a uniform medium such as neutral atomic hydrogen. The steady state solution which balances ionizations and recombinations results in a sphere of ionized hydrogen centered on the star. We have extended the model to allow for an evacuated, spherical cavity either centered on the star or with the star displaced with respect to the evacuated cavity. The resulting brightness distributions of a few representative geometries are illustrated and compared to actual H II regions of the Large Magellanic Cloud and the Milky Way. The extra degrees of freedom provided by our model allow it to approximate the actual H II regions better than a classic Strömgren sphere. Possible mechanisms to create the evacuated cavity are winds or supernovae.

1. INTRODUCTION

Bengt Strömgren (1939) created his eponymous sphere to explain the observations of Struve and Elvey of extended H II regions of the Milky Way observed in emission lines. The radius of a Strömgren sphere, r_s, associated with a star with Lyman continuum output, N_u, and ambient electron volume density, n_e, is determined by the balance of the rates of recombination (left-hand side) and ionization (right-hand side):

$$\alpha n_e^2 \frac{4\pi}{3} r_s^3 = N_u \,, \tag{1}$$

where α is a recombination coefficient.

Some H II regions resemble Strömgren spheres, but many do not. A dozen ionized gas regions of the Large Magellanic Cloud (LMC) are displayed in Figure 1. These examples were selected to illustrate that the morphologies predicted by the two-dimensional projections of the model presented in this paper are commonplace. The LMC examples show limb-brightened disks and also rings that are not symmetrically bright all around but have a "diamond ring" appearance, i.e., a ring with a bright point or a small arc of brightness along the edge of the ring.

This paper presents a simple geometrical variation on the Strömgren sphere model; for the sake of simplicity, it does not include the effects of dust, clumpiness, multiple stars, detailed radiative transfer, or dynamical effects. Such effects are reviewed by Yorke (1986). Our model is illustrated in Figure 2. We begin with a uniform medium, then evacuate a spherical cavity and insert a stationary, hot star anywhere inside the cavity. We solve for the steady state extent of the resulting asymmetric H II region in which ionization balances recombination. We render the emission measure for various geometries as viewed from various directions external to and very far from the H II region.

In nature the cavity might be created by mechanisms such as stellar winds or supernovae. The cavity could be created prior to or during the lifetime of the hot star that is emitting the ionizing photons. If the time to form a cluster or association of hot stars is long compared to the lifetime of the stars, then we expect that hot stars observed today will live in an environment in which an earlier generation of hot stars have created one or more cavities. Multiple cavities may tend to merge into a single one. New stars would be expected to form in the high-density medium on the edges of the evacuated cavity rather than its lower density interior. If these hypotheses for the clustering and sequential formation of hot stars are true, then conditions similar to those imagined in the modified Strömgren sphere model will naturally result.

The mechanism that shapes the ambient medium need not be the same as that which ionizes it now. In some of the examples presented here, shock ionization may contribute to the Hα brightness; from the Hα images themselves it is difficult to determine whether photoionization or shock ionization is the dominant mechanism. In the discussion of § 3, the importance of shock ionization relative to photoionization is important in the case of the Eridanus bubble (Heiles et al. 2000), not dominant for the Barnard loop (Heiles et al. 2000), and negligible for the Rosette Nebula (Menon 1962), and the extent to which it contributes in the LMC examples we do not know.

The modified case is not spherically symmetric but is cylindrically symmetric about the axis connecting the star

[1] Cottrell Scholar of Research Corporation.

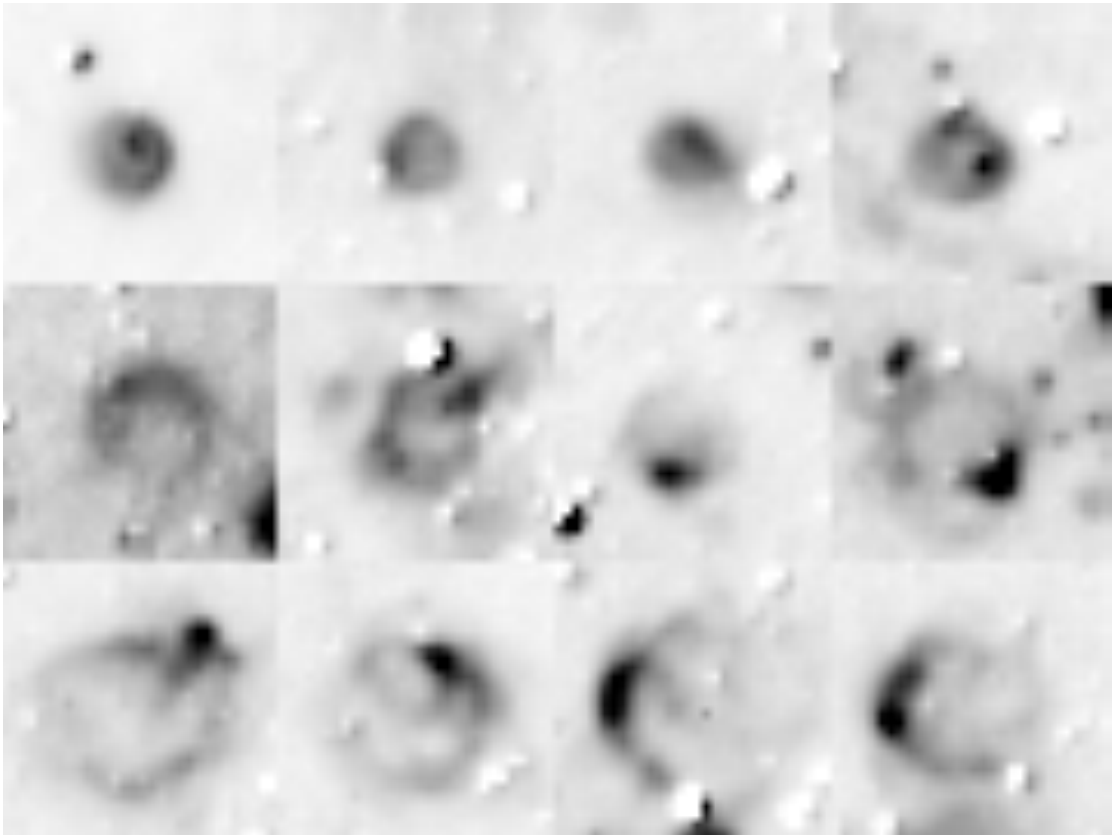

FIG. 1.—Ionized gas regions of the Large Magellanic Cloud illustrate that the morphologies that result from the modified Strömgren sphere model are commonplace. Each image is 24′ × 24′ (350 × 350 pc at a distance of 50 kpc). These images were extracted from the continuum-subtracted Hα image of Gaustad et al. (1999).

and the center of the evacuated sphere, i.e., CS in Figure 2. The distance to the inner edge of the H II region, r_i, is determined by geometry of the spherical cavity and the star's location in it. The radius of the outer edge of the H II region, r_o, is determined by equating the volume of the spherical shell enclosed between the inner edge and the outer edge to that of the Strömgren sphere of radius r_s:

$$r_o^3 - r_i^3 = r_s^3 \ . \tag{2}$$

The values or r_o and r_i are not constants but are functions of the direction in space away from the star, i.e., angle ϕ in Figure 2; r_s is a scalar constant for any particular model.

Because the medium's density is either zero or a constant value, the brightness distribution of emission measure, which depends on electron density squared, will be the same—except for a scalar—as that of a mechanism that depends on electron density to the first power or any other power.[2] Also, the brightness distribution of the modified sphere is scale invariant; we can consider the three lengths of equation (2) (r_o, r_i, and r_s) and the length d defined in Figure 2 as dimensionless quantities, normalized to the radius of the evacuated spherical cavity, r_c. In § 2 we refer to a parameter $\beta = r_s/r_c$, i.e., the ratio of the Strömgren radius to the radius of the cavity.

2. EXAMPLES

A representative array of modified Strömgren spheres is shown in Figures 3 and 4, which contain two-dimensional renderings of the surface brightness distributions as viewed from $\theta = 90°$ and 0°, respectively. The brightness is pro-

[2] In our model the density of the "evacuated cavity" is zero; in reality it is nonzero but is so much lower than the density of the ambient medium that its emission measure is negligible.

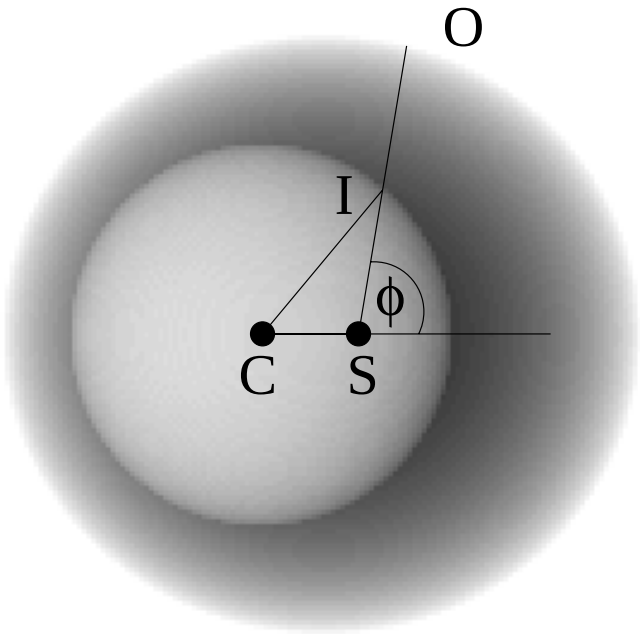

FIG. 2.—The modified Strömgren sphere has a star at S with the center of the evacuated sphere at C. The point I is at the inner edge of the ionized region, and O is at the outer edge. Lengths discussed in the text are r_i = SI, r_o = SO, r_c = CI, and d = CS. The angle ϕ is as shown.

portional to the path length of ionized gas along any line of sight; the distributions in Figures 3 and 4 were determined by numerically simulating the geometry on a 300^3 voxel array and then projecting the result according to the viewing angle θ. The leftmost columns of both Figures 3 and 4 are identical: they are spherically symmetric, modified Strömgren spheres for comparison with the other columns' models, each of which has its star displaced from its cavity's center.

The characteristics of the brightness distributions of the asymmetric models are described here. We describe the models viewed from $\theta = 90°$ first and those viewed from $\theta = 0°$ second. Unless noted otherwise, the descriptions in the next two paragraphs refer to the asymmetric examples in Figures 3 and 4, i.e., excluding the leftmost column of each.

For viewing angle $\theta = 90°$ (Fig. 3), the H II region is brighter on the side of cavity closer to the star and fainter on the opposite side of the cavity. The H II region extends farther to the left of the star than to its right, because photons stream across the cavity unimpeded. The opposite is true if the reference point is the center of the cavity rather than the star, because the star is displaced to the right of the cavity's center. For $\beta \gg 1$ the modified Strömgren sphere looks like a classic Strömgren sphere centered on the star with a depression in the brightness distribution caused by the cavity. For $\beta \approx 1$ our model can appear somewhat egg shaped. If the models are clipped below a specific value of surface brightness, they may appear crescent shaped. For $\beta \ll 1$ the model is either that of a thin spherical shell in the case where the star is near the center of the cavity, i.e., $d \ll r_c$, or if the star is near the edge of the cavity, i.e., $d \approx r_c$, the model's appearance is that of crescent-shaped "wings" extending to the left of a hemispherical H II region.

For viewing angle $\theta = 0°$ (Fig. 4), the brightness distributions are circularly symmetric. The $\beta \gg 1$ cases resemble classic Strömgren spheres even more than when viewed at angle $\theta = 90°$. An interesting effect occurs for $\beta \ll 1$ and $d \approx r_c$; this is approximately a blister H II region. From this viewing angle ($\theta = 0°$), the "approximately blister" model's brightness exhibits a local maximum on axis, then a local minimum farther out, followed by a ring of brightness immediately before the brightness goes to zero. We relate the blister case to the Orion Nebula in § 3.

For the spherically symmetric models, i.e., those illustrated in the leftmost columns of Figures 3 and 4, the radial brightness distribution is

$$I(r/r_c) = \begin{cases} \sqrt{(r_o/r_c)^2 - (r/r_c)^2} - \sqrt{(r_i/r_c)^2 - (r/r_c)^2}, & \text{if } r < r_c\,; \\ \sqrt{(r_o/r_c)^2 - (r/r_c)^2}, & \text{if } r_c \le r \le r_o\,; \\ 0, & \text{otherwise.} \end{cases} \tag{3}$$

The peak brightness occurs at the tangent point of the cavity, i.e., at $r = r_c$. The brightness increases with positive curvature up to the cavity's edge and decreases with negative curvature farther out, until it reaches zero at $r_o = \gamma r_c$, where $\gamma = (1 + \beta^3)^{1/3}$ and, as before, $\beta = r_s/r_c$. Some one-dimensional radial profiles of spherically symmetric models are plotted in Figure 5.

For a spherically symmetric, modified Strömgren sphere, the ratio of the on-axis surface brightness to the peak surface brightness is

$$I(r = 0)/I_{\text{peak}} = \sqrt{\frac{\gamma - 1}{\gamma + 1}}\,. \tag{4}$$

3. COMPARISONS WITH REAL H II REGIONS

The Rosette Nebula (=Sharpless 275 or NGC 2237-46) is a bright H II region with a ringlike appearance. The O5 star HD 46223 and the O6 star HD 46150 are the primary sources of ionization (Osterbrock & Stockhausen 1960) and are located near the center of the ring. The radial brightness distribution of the Rosette is plotted in Figure 5. Also plotted in Figure 5 are the radial profiles of four spherically

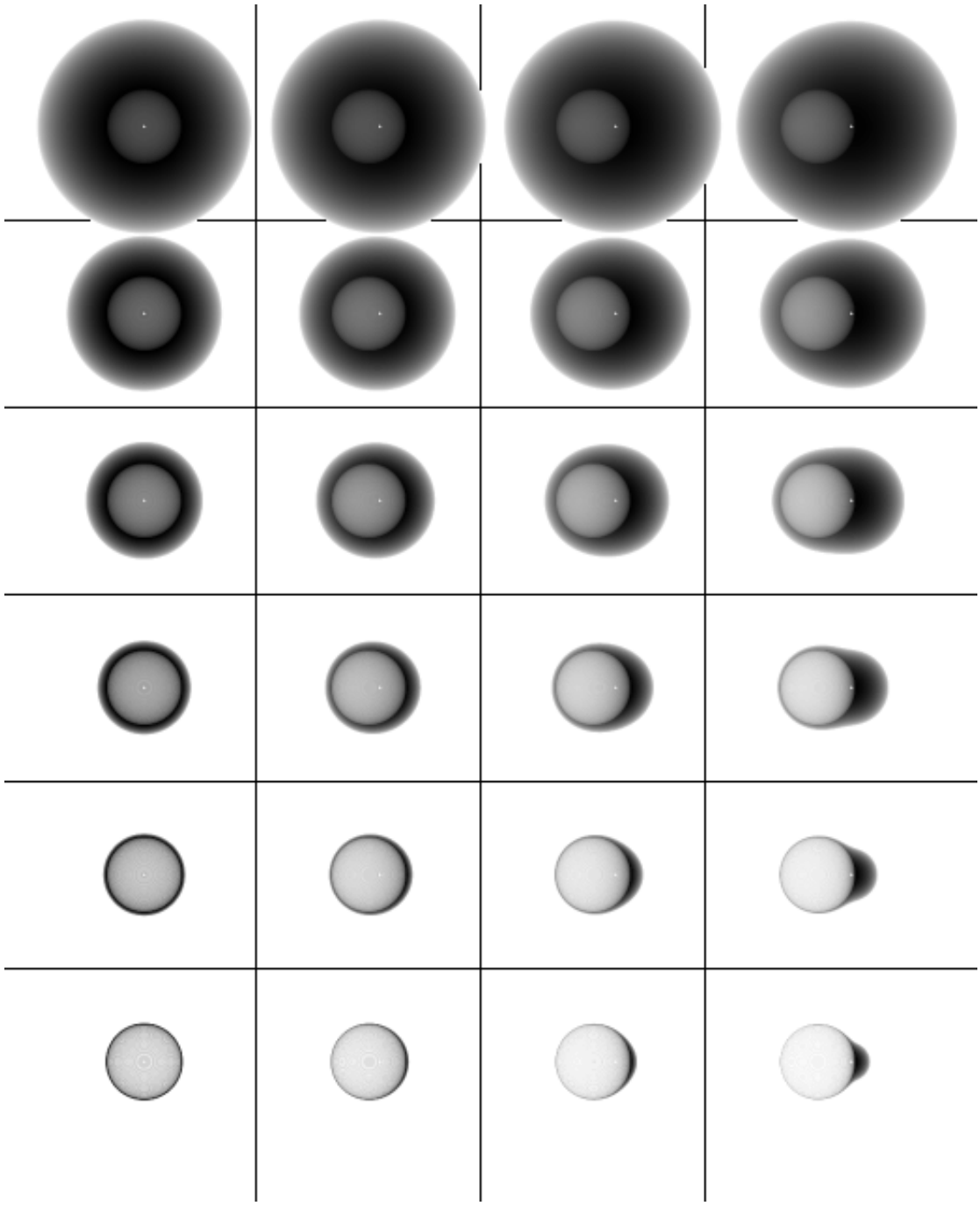

FIG. 3.—A representative array of modified Strömgren spheres is shown as viewed broadside, i.e., from an angle $\theta = 90°$. Each star is indicated by a white dot. The ratio of the Strömgren radius to the radius of the evacuated cavity, β, decreases down the page; the ratio of the distance of the star from the center of the evacuated cavity to the radius of that cavity, d/r_c, increases to the right. Values for β are 2.8, 2, 1.4, 1.0, 0.7, 0.5; values for d/r_c are 0.0, 0.3, 0.6, 0.9. Each model's brightness distribution is normalized to its individual peak brightness, and the gray scale is linear.

symmetric, modified Strömgren spheres. None of the spherically symmetric models fit both the interior and exterior simultaneously. In Hα, a $\beta = 1.4$ model fits the Rosette's interior distribution approximately, while a $\beta = 2.4$ model fits its exterior except for the faint, extended tail. In 10 cm radio continuum, a $\beta = 4$ model fits the interior approximately, and a $\beta = 2.4$ model fits the exterior. The new models presented here fit better than a classic Strömgren sphere in some ways. Both the new models and the Hα data show (*a*) a local minimum on axis, with (*b*) the brightness

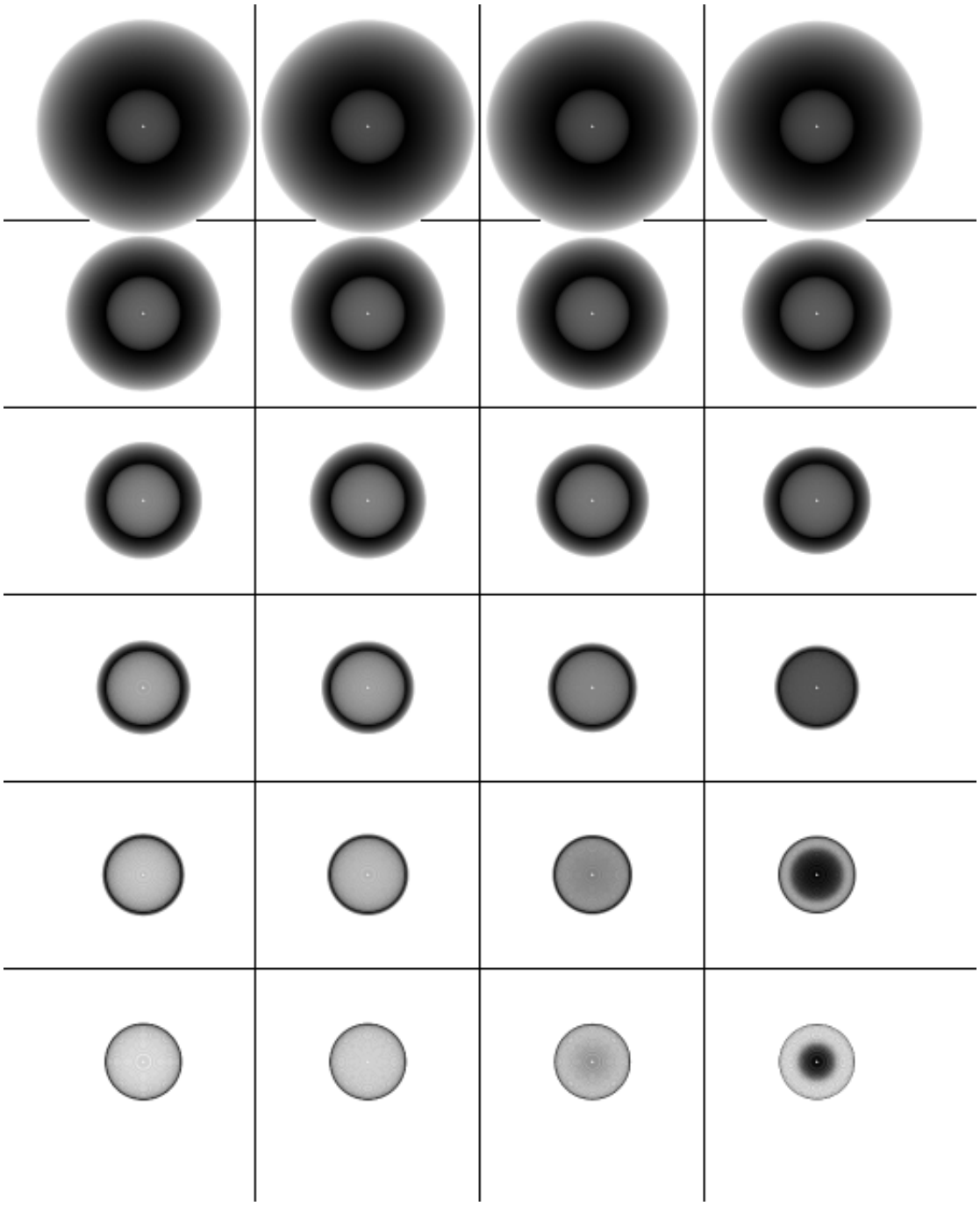

FIG. 4.—Same as Fig. 3 but viewed along the cylindrical symmetry axis, i.e., from an angle $\theta = 0°$. Note that except for the models in the left column, each star is displaced from the center of the evacuated cavity, even though its projection is on-axis for this viewing angle.

rising to a maximum with positive curvature, followed by (*c*) a decline with negative curvature. The radio brightness is similar to the Hα except that the radio brightness declines first with positive curvature and then with negative curvature. Items *a* and *b* are not features of the classic Strömgren sphere. The Rosette data have a long exponentially declining brightness distribution in Hα, i.e., a "tail" which neither this model nor the classic Strömgren sphere can reproduce. The radio data do not show such a tail, although that could be due to inadequate sensitivity or because the Hα data are contaminated by scattering. Topansa (2000) has shown that some of the Hα light of the periphery of the Rosette is not primary emission but reflection nebulosity. Using the radio data reproduced in Figure 5, Menon (1962) solved for the

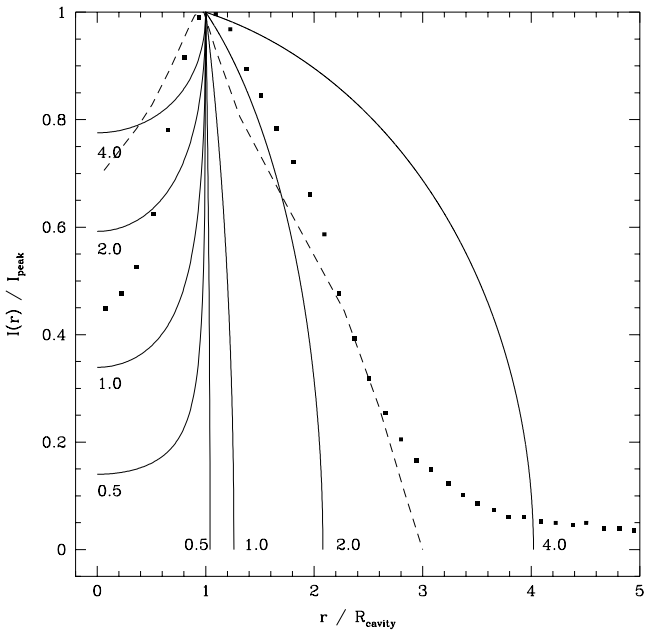

FIG. 5.—Radial cross sections of the surface brightness, $I(r)$, of four spherically symmetric, modified Strömgren spheres are plotted as solid lines. The curves are labeled with the ratio of the Strömgren radius to the radius of the cavity, denoted β in the text. Superposed is the mean radial surface brightness of the Rosette Nebula out to 80′ in Hα (*squares*; Celnik 1983) and out to 48′ in 10 cm radio continuum (*dashed line*; Menon 1962). Because of the 16′ beamwidth, the true radio brightness in the interior is steeper than plotted here.

radial electron density profile by assuming the nebula consists of a series of spherical shells. Menon's model is a more sophisticated version of our spherically symmetric modified Strömgren sphere, but in the end, our model is very similar to Menon's solution. Both have a sphere of near-zero density surrounded by a medium of nearly uniform density, with the outer ionization boundary due to lack of ionization rather than lack of matter.

The Orion Nebula has been modeled as a "blister" H II region, meaning an H II region that forms on the surface of a wall of neutral gas (Rubin et al. 1991). Characteristics of such a blister are an approximately hemispherical ionized region created in the wall, while ionizing photons from the hot stars stream nearly unimpeded in the direction away from the wall. In the limiting case of the Strömgren radius r_s being much smaller than the radius of the cavity r_c while d is approximately equal to r_c, our modified Strömgren sphere model approximates a blister geometry. A model with $\beta = 0.5$ and $d = 0.9r_c$ and viewed face-on (i.e., $\theta = 0°$) has a bright core surrounded by a bright outer ring (Fig. 4, *lower right*). This brightness distribution is like that of the Orion Nebula, with the bright core being M42, and one-half of the outer ring being Barnard's loop and the other half being the Eridanus bubble. That the radius of curvature of Barnard's loop is a few times smaller than that of the Eridanus bubble, and that the surface brightness of the former is much greater than the latter's, show that our model is too simple to be considered a model of the Orion/Eridanus region specifically, but it can help us visualize and understand the general characteristics of the region. An Hα image showing M42, Barnard's loop, and the Eridanus bubble can be found in Figure 4 of Heiles, Haffner, & Reynolds (1999). The Orion/Eridanus region is often given as an example of a champagne flow (Tenorio-Tagle 1982), with the great size of the Eridanus bubble compared to Barnard's loop explained as being the result of the greater density of the ambient medium toward the Galactic plane (i.e., on Barnard's loop's side) retarding the expansion of an evacuated cavity in that direction and allowing it to "blow out" away from the Galactic plane and creating the Eridanus bubble (e.g., Heiles, Haffner, & Reynolds 1999).

4. CONCLUSIONS

The Strömgren sphere does not describe true H II regions in all their natural complexity, but it provides a model of a physical situation, specifically a hot star in a uniform medium, without the confusing details of the true interstellar medium.

We have modified the physical situation by imagining that an evacuated cavity exists in the otherwise uniform medium and that the hot star is located within the cavity. The result is a cylindrically symmetric H II region whose shape depends on two parameters: the ratio of the Strömgren radius to the cavity's radius, and the ratio of the star's distance from the cavity's center to the radius of the cavity. The resulting H II region may take on various appearances depending on the viewing angle; examples are a limb-darkened disk with a central depression, an egglike shape, a crescent, a uniform ring, a "diamond-ring" shape, and a bright core with a ring around it. In one limiting case our model simplifies to the Strömgren sphere and in another our model simplifies to the blister geometry.

P. R. M. is supported in part by a Cottrell Scholarship from the Research Corporation and by the NSF CAREER award AST 98-74670. Figure 1 was created using data provided in FITS format by John Gaustad.

REFERENCES

Celnik, W. E. 1983, A&AS, 53, 403
Gaustad, J. E., Rosing, W., McCullough, P. R., & van Buren, D. 1999, in IAU Symp. 190, New Views of the Magellanic Clouds, ed. Y.-H. Chu, N. Suntzeff, J. Hesser, & D. Bohlender (San Francisco: ASP), 99
Heiles, C., Haffner, L. M., & Reynolds, R. J. 1999, in ASP Conf. Ser. 168, New Perspectives on the Interstellar Medium, ed. A. R. Taylor, T. L. Landecker, & G. Joncas (San Francisco: ASP), 211
Heiles, C., Haffner, L. M., Reynolds, R. J., & Tufte, S. L. 2000, ApJ, 536, 335
Menon, T. K. 1962, ApJ, 135, 394
Osterbrock, D. E., & Stockhausen, R. E. 1960, ApJ, 131, 310
Rubin, R. H., Simpson, J. P., Haas, M. R., & Erickson, E. F. 1991, PASP, 103, 834
Strömgren, B. 1939, ApJ, 89, 526
Tenorio-Tagle, G. 1982, in Regions of Recent Star Formation, ed. R. S. Roger & P. E. Dewdney (Dordrecht: Reidel), 1
Topansa, G. A. 2000, Ph.D. thesis, Virginia Polytechnic Inst.
Yorke, H. W. 1986, ARA&A, 24, 49